Weber Blockade Theory of Magnetoresistance Oscillations in Superconducting Strips

David Pekker,[1] Gil Refael,[1] and Paul M. Goldbart[2]

[1]*Department of Physics, California Institute of Technology, MC 114-36, Pasadena, California 91125, USA*
[2]*School of Physics, Georgia Institute of Technology, 837 State Street, Atlanta, Georgia 30332-0430, USA*

(Received 22 October 2010; published 30 June 2011)

Recent experiments on the conductance of thin, narrow superconducting strips have found periodic fluctuations, as a function of the perpendicular magnetic field, with a period corresponding to approximately two flux quanta per strip area [A. Johansson *et al.*, Phys. Rev. Lett. **95**, 116805 (2005)]. We argue that the low-energy degrees of freedom responsible for dissipation correspond to vortex motion. Using vortex-charge duality, we show that the superconducting strip behaves as the dual of a quantum dot, with the vortices, magnetic field, and bias current respectively playing the roles of the electrons, gate voltage, and source-drain voltage. In the bias-current versus magnetic-field plane, the strip conductance displays regions of small vortex conductance (i.e., small electrical resistance) that we term ''Weber blockade'' diamonds, which are dual to Coulomb blockade diamonds in quantum dots.

DOI: 10.1103/PhysRevLett.107.017002 PACS numbers: 74.78.−w, 73.21.La, 74.40.−n

Introduction.—It is often effective to characterize strongly correlated quantum systems in terms of the emergent, collective freedoms that describe their low-energy behavior. Vortices in superconductors constitute the most prominent example of such freedoms. The unbinding of such vortices leads to the Berezinskii-Kosterlitz-Thouless phase transition exhibited by thin-film superconductors [1], and is widely suspected to be a feature of the superfluid-insulator quantum phase transition—exhibited by a number of systems [2–4], particularly granular InO films [5,6].

Magnetoresistance oscillations, starting with the Little-Parks effect [7], are a well-known feature of superconductivity and, in particular, of mesoscopic superconducting devices; see, e.g., [8]. Motivated by recent experiments by the Shahar group on superconducting InO strips [9], in this Letter we address such magnetoresistance oscillations from the vortex as opposed to the electron (i.e., charge) point of view. By using charge-vortex duality, we show that the notion of a ''vortex blockade'' allows us to explain such oscillations, in analogy with the Coulomb blockade theory that has been applied widely to electron passage through quantum dots. We also find a series of ''Weber'' diamonds, which are analogs of the Coulomb blockade diamonds, except for the important distinction that the electrical conductivity is maximal (rather than minimal) inside the Weber diamonds. The charge-vortex duality allows us to make direct use of the sophisticated formalism developed to quantitatively account for quantum dynamical effects in quantum dots. Below, we apply the Beenakker formalism of dissipative quantum-dot transport [10], with the dissipation taking place via the normal modes of the vortex medium in the strip. Within this model of dissipation, we predict that the resistivity of the strip should be activated inside the diamonds and have a power-law falloff outside. Finally, we compare our results with experiments.

Setup.—We are concerned with describing the current-voltage characteristics of a superconducting strip that is subject to a perpendicular magnetic field. The setup [see Fig. 1(a)] consists of a superconducting strip, contacted via a pair of leads that are used to inject a supercurrent into the strip. The voltage across the strip is read out using the same leads, and we assume that the dissipation probed originates entirely in the superconducting strip.

We make several restrictions on the strip geometry pertaining to vortices. First, we assume that the strip thickness $\lesssim \xi$, where ξ is the coherence length. This assumption ensures that the vortices are of pancake (Pearl) type, as opposed to line vortices [11]. Second, based on magnetic force imaging [12], we assume that the strip is narrow, in the sense that vortices always lie in a line along the strip center, like peas in a pod. In strips wider than $\approx 5\xi$, vortices tend to form Abrikosov-like lattices at higher fields. We shall address the question of wider strips in a separate article. Finally, we comment that we consider the strip to be free of vortex pinning sites, and also to be of finite length (in practice [9], $\sim 10\xi$–100ξ) so that configurations having distinct numbers of vortices have sufficiently different energies as compared to $k_B T$.

Dual description of a superconducting strip.—Via charge-vortex duality, we map the behavior of a superconducting strip onto that of a quantum dot capable of undergoing a Coulomb blockade, as defined in Fig. 1(b) and its caption. The origin of dissipation in the dual picture is the Magnus force, due to the bias supercurrent, on the vortices. This force creates a potential difference between the vacua on either side of the strip, and thus it acts as the source-drain bias of the dot does. The transport of vortices across the superconducting strip has a direct consequence for electrical transport within the strip, viz., each time a vortex passes across the strip, the phase between the left and right leads changes by 2π. The voltage V between the leads is given by the Josephson relation $V = \Phi_0 \Gamma_N$, where Γ_N is the net rate of vortex tunneling and $\Phi_0 \equiv h/2e$ the superconducting flux quantum.

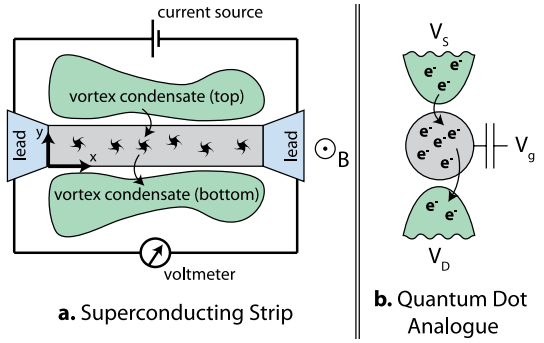

FIG. 1 (color online). (a) Schematic: superconducting strip (gray) is immersed in a magnetic field B pointing out of the plane of the strip. The strip is contacted via a pair of leads (blue) that are used to both supply a bias supercurrent J and measure the voltage V. Vortices (depicted by swirls) reside in the strip, but occasionally traverse the strip (cf. the vortex trajectory indicated by arrows). Via the Josephson relation, such crossings correspond to voltage spikes and thus dissipation. (b) Analogous quantum-dot circuit. The dot is depicted by the gray disc. The vortices and the magnetic field in the strip correspond, respectively, to the electrons and the gate voltage V_g of the dot. The source and drain for the vortices are the vacua adjacent to the strip. As the vacua do not a have well-defined number of vortices, we describe them as vortex condensates (green) of well-defined phase, with the potential energy difference between the condensates set by the bias supercurrent. Thus, J in the vortex analogy corresponds to the source-drain voltage $V_S - V_D$ in the dot.

Having defined the analogy, we split the problem of computing the vortex conductance (i.e., the electrical resistance) of the strip into two subproblems. The first consists of describing the energetics of static configurations of distinct numbers of vortices. The second consists of utilizing the vortex energetics to construct a master equation describing vortex hopping. In constructing the master equation we make the typical—and experimentally relevant—assumption that vortex tunneling rates Γ_t (Γ_b) between the strip and the top (bottom) vortex reservoirs are the smallest energy scales in the system, i.e., Γ_t, $\Gamma_b \ll k_B T$. This assumption ensures that after a vortex tunnels onto the strip it is completely dephased before it is likely to tunnel again, validating the use of the master equation.

Vortex energetics.—We describe the strip using the phase-only model Hamiltonian

$$H = (\rho/2)\int dxdy|\nabla\phi - (2\pi/\Phi_0)\boldsymbol{A}|^2, \qquad (1)$$

in which $\rho \sim k_B T_{\mathrm{BKT}}$ is the superfluid stiffness, ϕ is the phase of the order parameter, and $\boldsymbol{A} = -B(y - w/2)\hat{\boldsymbol{e}}_x$ is the vector potential in the London gauge. We use a coordinate system in which y runs from 0 to w across the width of the strip and the long direction of the strip runs in the x direction, Fig. 1(a). We use the boundary conditions $\nabla_y\phi|_{y=0,w} = 0$ and $\phi(x, y) = \phi(x + L, y)$. Although the boundary conditions at the interface with the leads depend on microscopics, any choice of boundary conditions that preserves the discreteness of the vortex "charging" energy would result in magnetoresistance oscillations, and thus we use periodic boundary conditions. Next, we obtain the single- and intervortex energetics.

The potential energy of a single vortex in a strip, as a function of its position y across the strip, was thoroughly explored [13]. The results consist of four parts. (i) The vortex core energy E_{core}. (ii) The energy of interaction of the vortex with its images, $E_{\mathrm{image}} = -2\pi\rho\ln[\sin(\pi\xi/w)/\sin(\pi y/w)]$, where the ln divergence due to the closest image is cut off by vortex core length scale ξ. In further calculations we shall absorb the vortex core energy into the cutoff length scale. (iii) The interaction of the vortex with the magnetic field, i.e., $E_{vB} = (2\pi)^2(\rho B/\Phi_0)[(y - w/2)^2 - (\xi - w/2)^2]$. (iv) The potential due to the Magnus force, i.e., $E_{\mathrm{Magnus}} = \Phi_0(J/w)(y - w/2)$, where J is the bias current.

The consequences of these four parts are summarized in Fig. 2(a), in which we plot the potential energy of a single vortex in an infinitely long strip, as a function of its position. For small applied magnetic fields, vortices are unstable everywhere inside the strip. For larger magnetic fields, the configuration having a vortex trapped in the middle of the strip becomes metastable. At a still larger field (i.e., the lower critical field) the vortex becomes stable, globally. A bias current along the strip produces a tilting of the vortex potential energy [see Fig. 2(b)].

To find the interaction energy between vortices, described by Eq. (1), we use the conformal mapping $z = x + iy = \exp(\pi u/w)$ to identify the strip $0 < \mathrm{Im}u < w$ with the upper half-plane $0 < \mathrm{Im}z < \infty$. The phase field of a vortex located at $z_0 = x_0 + iy_0$ in the upper half-plane can be found using a single image vortex: $\phi(z; z_0) = \mathrm{Im}[\ln(z - z_0) - \ln(z - z_0^*)]$. Using the Cauchy-Riemann equations, we identify the vortex potential $G_{\text{half-plane}}$ as the real part of the harmonic function, the imaginary part of which corresponds to the vortex phase field. Applying the conformal mapping to $G_{\text{half-plane}}$, we find the potential of a vortex in the strip

$$G_{\mathrm{strip}}(u; u_0) = 2\pi\rho_s \mathrm{Re}\left[\ln\frac{e^{\pi u/w} - e^{\pi u_0/w}}{e^{\pi u/w} - e^{\pi u_0^*/w}}\right], \qquad (2)$$

and the intervortex energy $E_{vv} = \frac{1}{2}\sum_{i\neq j} G_{\mathrm{strip}}(u_i; u_j)$.

Vortex blockade.—We begin by examining the Weber (cf. Coulomb) blockade in the absence of a bias current (cf. source-drain voltage). The key to either blockade is that for generic values of the magnetic field B (cf. gate voltage V_g) the energies for N or $N + 1$ vortices (cf. electrons) to be on the strip (dot) differ, and therefore vortex (cf. charge) current is impeded. However, for special values of B (cf. V_g), the degeneracy condition

$$E_N(B, J = 0) = E_{N+1}(B, J = 0) \qquad (3)$$

is met, allowing vortices (cf. electrons) to move freely on to and off of the strip (cf. dot), thus lifting the blockade.

For the case of nonzero bias current J, we must consider separately the processes of adding vortices from the top

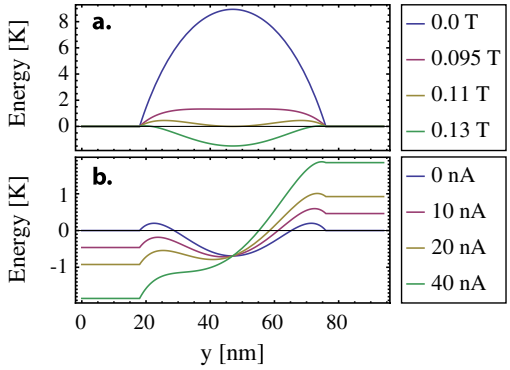

FIG. 2 (color online). (a) Vortex potential energy vs its position across the strip for various magnetic fields for a 94 nm wide strip with $\xi = 18$ nm and $\rho = 5$ K, (see Ref. [13]). (b) Same as (a), but with nonzero bias current along the strip and magnetic field fixed at 0.12 T. Note the energy barriers near the strip edges for small fields and currents.

and bottom reservoirs. These considerations furnish two stability conditions, viz.,

$$E_N(B, J) + E_{\text{top/bottom}} = E_{N+1}(B, J), \tag{4}$$

that define the Weber diamonds, in which E_{top} and E_{bottom} are the potentials of the top and bottom reservoirs. In Fig. 3, we plot the first few diamonds in the J vs B plane. The regions inside the diamonds correspond to 1, 2, ... vortices on the strip in the blockaded regime (i.e., poor vortex conduction across, and therefore good electrical conduction along, the strip). For increased bias currents, the potential difference between the vortex reservoirs overcomes the blockade, driving the strip into the good vortex-conduction regime (i.e., to poor electrical conduction along the strip).

Master equation.—In order to estimate the actual magnitude of the conductance of the superconducting strip, we need to extend the static model of the blockade to include the dynamics of vortex hopping and energy dissipation. For the quantum-dot case, dissipation arises in the leads, which act as "decohering baths" in which the quasiparticles are assumed always to obey the Fermi-Dirac distribution [10]. In the vortex case, dissipation occurs not in the vortex reservoirs but in the strip itself. However, there are many

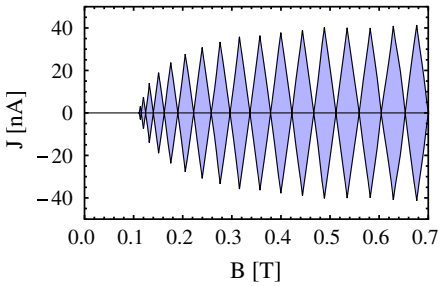

FIG. 3 (color online). Weber diamonds in the bias-current vs magnetic-field plane ($w = 94$ nm, $L = 1$ μm, $\xi = 18$ nm, and $\rho = 5$ K). Regions inside the diamonds correspond to small electrical resistance along the superconducting strip or, equivalently, to small vortex conductance across it.

possible damping mechanisms, such as coupling to the bath of Bogoliubov quasiparticles. The question of which mechanism dominates depends on the microscopic properties of the superconductor. We shall focus here on the simplest possibility: that the thermal bath consists of the normal modes of the line of vortices inside the strip. For narrow strips, the vortices act as hard-core bosons, with a single gapless excitation mode described by the Tomonaga-Luttinger (TL) model.

For the coupling between the vortex reservoirs and the vortices inside the strip we introduce a model Hamiltonian that accounts for vortex tunneling between them:

$$H_{\text{tun}} = \int dx b(x)(t_t e^{i\theta_t} + t_b e^{i\theta_b}) + \text{H.c.}, \tag{5}$$

where $b(x)$ is the operator that annihilates a vortex at position x along the strip center. Following Beenakker's approach to quantum dots [10], which invokes Fermi's golden rule, we obtain a master equation for the probabilities $P_0, P_1, \ldots$ of having $0, 1, \ldots$ vortices on the strip:

$$\partial_t P_N = \sum_{\omega,\sigma,\alpha} P_{N+\sigma} T_{N+\sigma\to N}(\omega)\gamma_\alpha \delta_{E_{N+\sigma}-E_N-\sigma\mathcal{E}_\alpha+\omega} - \sum_{\omega,\sigma,\alpha} P_N T_{N\to N+\sigma}(\omega)\gamma_\alpha \delta_{E_N-E_{N+\sigma}-\sigma\mathcal{E}_\alpha+\omega}, \tag{6}$$

where $\sigma = \pm 1$, $\alpha \in \{t, b\}$, $\mathcal{E}_t$ and $\mathcal{E}_b$ are the potentials of the top and bottom vortex reservoirs, the δ functions account for energy conservation, and $\gamma_\alpha = t_\alpha^2 N$ is the vortex tunneling coefficient in which N accounts for the number of positions at which the vortex can tunnel. The matrix elements $T_{N\to N\pm 1}(\omega)$ correspond to adding or subtracting a vortex from the TL liquid of vortices in the strip at frequency ω:

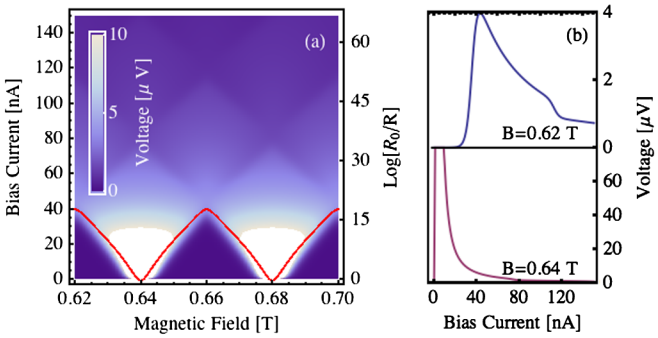

FIG. 4 (color online). Structure of a typical Webber diamond of Fig. 3 at temperature of 0.1 K (and tunneling amplitude of 0.1 K): (a) Map of the voltage across the strip as a function of magnetic field and bias current. Superposed on the map (red curve) is $\ln[R_0/R(B)]$, i.e., the logarithm of the zero-bias resistance as a function of magnetic field ($R_0 = 163$ kΩ). (b) V-I characteristic of the strip at two values of the magnetic field: in the middle of a diamond (top) and between two diamonds (bottom). At small biases there is, in both cases, an initial linear response, followed by activated behavior inside the diamond, and finally a universal power-law decay with secondary diamonds superposed on it.

TABLE I. Coherence length ξ (a fitting parameter) required to reproduce the experimentally measured period P using our theoretical model for four samples [15] of widths w and lengths L (Table I of Ref. [9]). In each case, we fit the experimental period at the intermediate value of magnetic field $B \approx 1.5$ T. For comparison, we also provide the geometric period $P_{\text{geometric}} = (\Phi_0 wL)^{-1}$. For all samples, we find reasonable values for ξ, which should lie between 10 and 30 nm [9].

sample	w [nm]	L [μm]	P [T]	$P_{\text{geometric}}$ [T]	ξ [nm]
39Ue	40	1.5	0.083	0.034	10
86Gc	94	1.0	0.048	0.022	17
86Gd	94	1.0	0.046	0.022	16
86Ge	94	1.0	0.043	0.022	15

$$T_{N\to N\pm 1} = [n_B(\omega) + 0.5 \pm 0.5]A_N(\omega), \qquad (7)$$

where $n_B(\omega)$ is the Bose function and $A_N(\omega) = 2\text{Im}G(\omega + i\delta, k = 0)$ is the zero-momentum spectral function of the TL liquid with N vortices [14].

Using our TL liquid model of dissipation, we investigate the structure of a typical Weber diamond for the strip parameters of Fig. 3. In Fig. 4(a), we plot the map of the voltage as a function of B and J. The map indicates that, even at reasonable temperatures, there is a critical bias current $J_c(B)$ above which the blockade is broken and the voltage rises. $J_c(B)$ can be clearly seen in the V-I characteristics, which show an activated behavior inside the diamond [Fig. 4(b)]. Comparing $J_c(B)$ with the zero-bias resistance $R(B)$, we see that $R(B) \sim e^{-J_c(B)/E}$, where the energy scale $E \approx k_B T$.

Comparison with experiment.—Using Eq. (3), we can estimate theoretically the period of the magnetoresistance oscillations for the sample geometries of Ref. [9]. The only undetermined parameter in the estimate is ξ. Treating ξ as a fitting parameter, we were able to fit the periods of all four narrow-strip samples (Table I). We remark that the experimentally observed period is always longer than the geometric period associated with adding a flux quantum to the area of the strip (Table I). Our theory implies that the effective width is narrower than the geometrical width, due to the strong attraction of vortices to the strip edges by their images (i.e., E_{image}), thus resolving the period puzzle. The experimental signal shows only mild magnetoresistance oscillations, rather than the pronounced vortex-blockade peaks that we predict. We suspect that this smearing is a result of Γ_t and Γ_b being large, and thus the strip operating in between the open- and closed-dot regimes. Alternatively, the smearing may be a result of thermal broadening. If so, lowering the temperature should strengthen the blockade features.

Concluding remarks.—We have demonstrated that magnetoresistance oscillations in superconducting strips can be readily described using vortex—as opposed to Cooper-pair or charge—coordinates. Via an analogy with the physics of quantum dots, we have constructed a model for the Weber blockade of a superconducting strip that captures the essential features of the magnetoresistance oscillations observed experimentally. The exact dissipation mechanism remains to be understood; it will determine the shape of the Coloumb blockade peaks predicted in Eq. (6) but not the magnetoresistance period. Alternatively, one could use the experimental blockade signatures to investigate the nature of dissipation.

We thank D. Shahar and J. Meyer for useful discussions, and the Aspen Center for Physics for its hospitality. This work was supported by DOE DE-FG02-07ER46453 (PMG), the Research Corporation, Packard and Sloan Foundation (G. R.), and the Du Bridge Foundation (D. P.).

Note added.—Concurrent work by Y. Atzmon and E. Shimshoni considers magnetoresistance oscillations from a complementary point of view [16], and arrived at similar conclusions.

[1] V. L. Berezinskii, Sov. Phys. JETP **34**, 610 (1972); J. M. Kosterlitz and D. J. Thouless, J. Phys. C **6**, 1181 (1973).
[2] A. Yazdani and A. Kapitulnik, Phys. Rev. Lett. **74**, 3037 (1995).
[3] N. Marković, C. Christiansen, A. M. Mack, W. H. Huber, and A. M. Goldman, Phys. Rev. B **60**, 4320 (1999).
[4] N. Mason and A. Kapitulnik, Phys. Rev. B **64**, 060504 (2001).
[5] R. Crane *et al.*, Phys. Rev. B **75**, 184530 (2007).
[6] D. Kowal and Z. Ovadyahu, Physica C (Amsterdam) **468**, 322 (2008).
[7] W. A. Little and R. D. Parks, Phys. Rev. Lett. **9**, 9 (1962).
[8] See, e.g. K. Yu. Arutyunov and T. T. Hongisto, Phys. Rev. B **70**, 064514 (2004); A. Kanda, B. J. Baelus, F. M. Peeters, K. Kadowaki, and Y. Ootuka, Phys. Rev. Lett. **93**, 257002 (2004); B. J. Baelus *et al.*, Phys. Rev. B **73**, 024514 (2006); N. Schildermans *et al.*, Phys. Rev. B **76**, 224501 (2007).
[9] A. Johansson *et al.*, Phys. Rev. Lett. **95**, 116805 (2005).
[10] C. W. J. Beenakker, Phys. Rev. B **44**, 1646 (1991); see also G.-L. Ingold and Yu. V. Nazarov, in *Single Charge Tunneling*, edited by H. Grabert and M. H. Devoret (Plenum, New York, 1992), Chap. 2.
[11] J. Pearl, Appl. Phys. Lett. **5**, 65 (1964).
[12] G. Stan, S. B. Field, and J. M. Martinis, Phys. Rev. Lett. **92**, 097003 (2004).
[13] K. K. Likharev, Sov. Radiophys. **14**, 722 (1973); see also J. R. Clem, Bull. Am. Phys. Soc. **43**, 411 (1972); G. M. Maksimova, Phys. Solid State **40**, 1607 (1998).
[14] See, e.g., T. Giamarchi, *Quantum Physics in One Dimension* (Claredon Press, Oxford, 2004), Appendix C.
[15] We do not fit sample 5 of Ref. [9] as it is too wide for treatment in terms of our narrow-strip theory.
[16] Y. Atzmon and E. Shimshoni, arXiv:1010.0664 [Phys. Rev. B (to be published)].